RAMANUJAN-DERIVED HYPERGEOMETRIC FUNCTIONS DESCRIBE HIDDEN COUPLED DYNAMICS IN PHYSICAL AND BIOLOGICAL SYSTEMS

Arturo Tozzi
Center for Nonlinear Science, Department of Physics, University of North Texas, Denton, Texas, USA
1155 Union Circle, #311427 Denton, TX 76203-5017 USA
tozziarturo@libero.it

ABSTRACT

Ramanujan's real period functions plus Picard–Fuchs differential equations and Gaussian hypergeometric functions generate a wide range of simple hypergeometric manifolds (henceforward PFHM) consisting of two-dimensional coupled subsystems combined in a single three-dimensional system with dihedral symmetry. We argue that PFHM could be used to elucidate the homoclinic paths equipped with stable, closed and constrained orbits that characterize the dynamical behavior of a large number of physical and biological systems. Since PFHM encompasses coupled subsystems with Hamiltonian interactions that are reciprocal in nature, the options for the total system's energetic conformation are restrained. Therefore, energetic changes in a subsystem are inversely correlated with energetic changes in another subsystem. This balanced, inverse energetic reciprocity could be used to elucidate the unusual behavior of quantum entangled particles and the thermodynamic constraints dictating the final shape of frustrated proteins. Also, the thermodynamic paths of apparently isolated systems can be influenced by feedback mechanisms from hidden subsystems that exert their influence and can be quantified, even without full knowledge of every control parameter. PHFM can be methodologically treated in terms of cycle attractors, shedding new light on well-known physical phenomena like the dynamical behavior of monostatic bodies. Yet, the possibility to analyze two-dimensional paths in terms of three-dimensional routes could be useful to assess the ubiquitous occurrence of the Turing's reaction-diffusion model in biological systems. We suggest that PFHM might stand for a general mathematical apparatus shaping the phase space of various real dynamical paths, with applications in digital imaging, cryptography and memory storing.

KEYWORDS: gomboc; quantum entanglement; dynamical systems theory; graphene; atom.

INTRODUCTION

Differential equations' multivariable functions and their partial derivatives drive the energetic behavior of various dynamical paths, from logarithmic to exponential behaviors, from limit cycle to Lorentz-like attractors. We suggest to use the Picard–Fuchs equation (henceforward PF) and its variants to investigate the energetic constraints of physical and biological dynamical systems. PF is a simple, linear, ordinary differential equation whose solutions describe the periods of elliptic curves (Shen 2017). PF allows the evaluation of integrals without resorting to direct integration techniques, providing. e.g., a computationally simple method of calculating higher-order quantum-mechanical corrections to the classical action (Kreshchuk and Gulden, 2019). PF has the unvaluable advantage of encompassing period-energy functions, so that the energy can be used as a parameter.

PF can be can be also written in terms of second-order differential equations based on the Gaussian hypergeometric function ${}_2F_1$ (a,b;c;z), i.e., a special function characterized by three regular singular points where the growth of solutions in the complex plane is bounded by an algebraic function (Becken and Schmelcher, 2000; Olde Daalhuis 2010). Hypergeometric differential equations represent solutions of many physical problems like, e.g., the Schrödinger equation for the hydrogen atom and the harmonic oscillators analyzed in terms of Hermite polynomials (Ratner et al., 2001; Jong et al., 2015). The hypergeometric version of PF is satisfied by a set of integral period functions leading to geometries characterized by simple, plane curves that are closed and start at regular points (Beukers and Heckman, 1989; Fürnsinn and Yurkevich, 2023). Simple and manageable PF-derived hypergeometric manifolds (henceforward PFHM) are achieved (**Figure 1**), characterized by a doubly periodic elliptic function and by a countable toric section of the Hamiltonian (Klee 2018a). A fixed value of the Hamiltonian can be used to specify the coordinates of a particular particle trajectory inside PFHM. Given the system's Hamiltonian $H(p, q)$, the associated real period function $T(\alpha)$ can be described by integral-differential algorithms (Klee 2019):

$$T(\alpha) = {}_2F_1\left(\frac{1}{2}, \frac{s-1}{s}; 1; \alpha^2\right),\ s = 3, 4, \text{ or } 6$$

with the same signatures $s \in \{2, 3, 4, 6\}$ that can be found in the Ramanujan theory of elliptic functions related to the integral period functions K_1, K_2 and K_3 (Ramanujan 1914; Shen 2017).

When the potential reaches a minimum, the phase curves become loops that can be measured by the period function $T(\alpha)$ (Klee 2019):

$$T(\alpha) = \oint dt = \oint dq / p(\alpha, q)$$

The invariant differential $dt = dq / p$ can be integrated on any loop around the Riemannian surface $\alpha = 2H(p, q),\ (q, p) \in \mathbb{C}^2$

PFHM is a versatile tool that generates many algorithms and different series of identities (Klee 2018a). Slight changes in the variable period T(α) and/or the Gaussian hypergeometric function produce fully different manifolds that can be interpreted in terms of (physical or biological) dynamical systems featuring dihedral symmetry (**Figure 1**). Notably, the systems' energetic requirements and constraints can be calculated by plotting cross sections of the toric energy surface with plane curves. In the sequel, we will assess the phase space and the Hamiltonian of dynamical systems characterized by stable and closed orbits, with special emphasis on their energetic features.

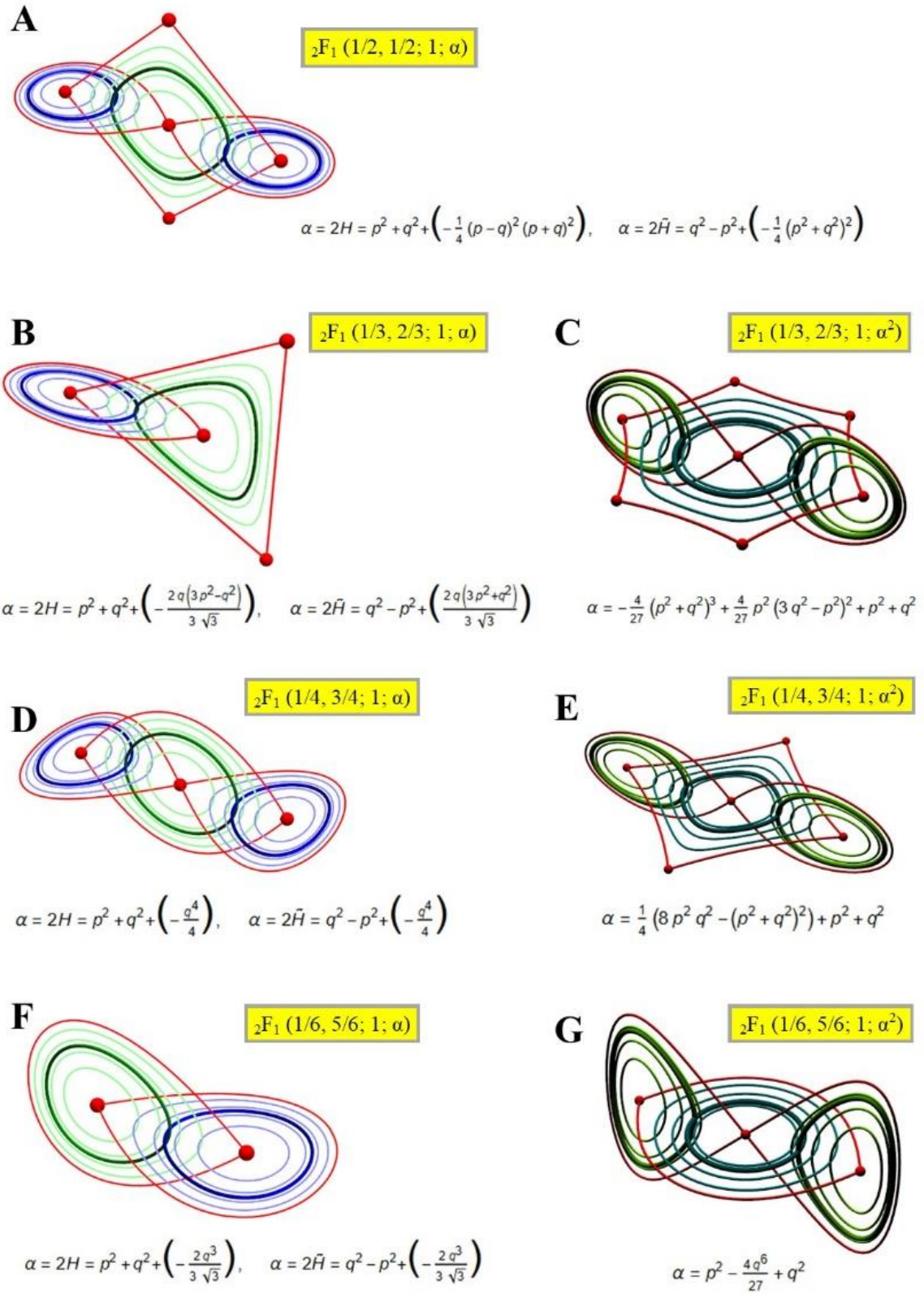

Figure 1. Hypergeometric Picard-Fuchs equations generate dynamical systems featuring dihedral symmetry with different phase space's conformations. At a fixed value of energy α = 0.469, slight modifications in the real period function T(α) (described in the yellow squares) lead to the production of various hypergeometric manifolds with different toric sections of the Hamiltonian. Modified from Klee (2018a); Klee (2019).

FROM HYPERGEOMETRIC PHASE SPACES TO REAL PHYSICAL AND BIOLOGICAL SYSTEMS

We argue that PFHM and the Ramanujan's derived real period functions could be used to elucidate real systems' phase spaces and energetic dynamics. PFHM might stand for the mathematical counterpart of various physical and/or biological dynamical paths. To provide a proof-of-concept example, we examine here the phase space trajectories of an isolated two-dimensional system S1 characterized by homoclinic, stable, closed orbits (**Figure 2A**). Period integrals along the contour curves enable the evaluation of the S1's time dynamics (Klee 2018b). The S1's planar layer contains a family of Hamiltonian level curves indexed by energy $\alpha \in (0, 1)$ with the lowest energetic level located at the center and the higher on the borders. The higher the energy, the larger the closed orbit crossed by a hypothetical particle traveling in the S1's phase space.

The next step is to consider S1 not anymore as isolated, rather as a subsystem coupled with another hidden two-dimensional subsystem, say S2, equipped with the same homoclinic, stable, closed orbits. The features of such S1-S2 system are illustrated in **Figure 1F** and **Figures 2B-E**. The HPFM procedure allows S1 and its family of Hamiltonian curves to be coupled with S2 Hamiltonian curves that reciprocally influence each other. The system formed by the two subsystems S1 and S2 displays peculiar features:

1) The subsystems are coupled inside a single complex dynamical system described by the PFHM dictates.
2) The two-dimensional subsystems are located on perpendicular planes inside a three-dimensional phase space.
3) The system features dihedral symmetry.
4) The system is finite.
5) The constrained trajectories of the subsystems follow homoclinic, stable and closed orbits.
6) The system could be treated either as continuous or quantized.
7) Due to the extreme value theorem, a real-valued function that is continuous on the closed and bounded interval must attain at least a maximum and a minimum on a compact manifold.
8) Plotting cross sections of the toric energy surfaces allows energy inversion symmetry. Differently from other Hamiltonian surfaces, the real period T(α) determines the complex period T(1-α) up to a rescaling, leading to energy inversion $\frac{\alpha}{1-\alpha}$ (Klee 2018a).
9) Contrary to S1, the S2 energetic values decrease from the center to the periphery.
10) For every fixed value of the Hamiltonian, equipotential subspaces can be found in every subsystem. Therefore, changes in radius and energetic levels in S1 are inversely and correlated with changes in radius and energetic levels in S2 (**Figures 2B-D**).
11) The (physical or biological) subsystems S1 and S2 are coupled is such a way that the total energy of the system must be preserved. In accordance with the principle that for every action there is an equal and opposite reaction, energetic increases in S1 must be balanced by inversely proportional energetic decreases in S2, and vice versa.

Summarizing, we argue that PFHM could describe real physical and/or biological systems in which the energetic changes occurring in the subsystem under evaluation are linearly correlated with the energetic changes occurring in hidden coupled subsystems.

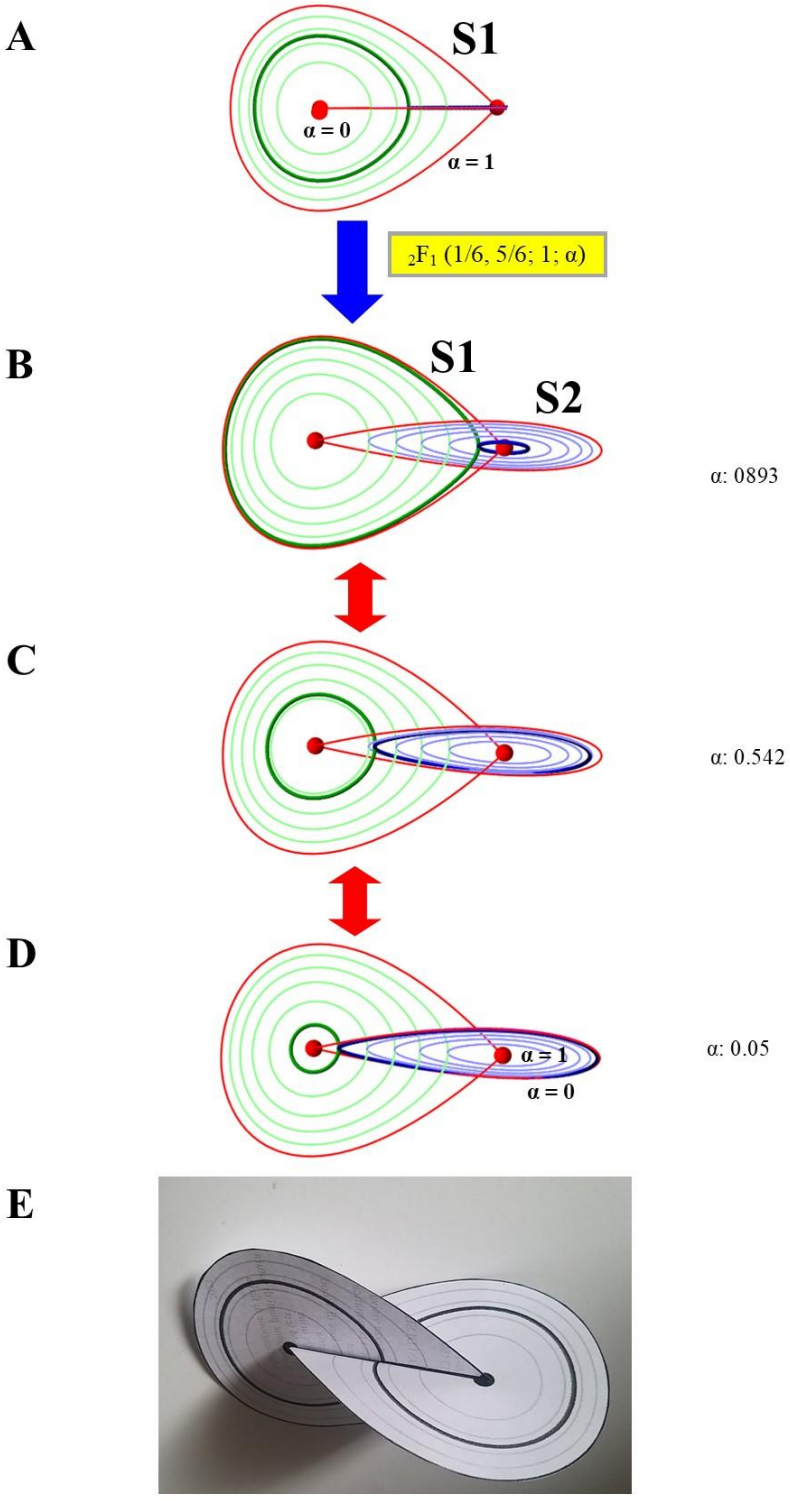

Figure 2. The dynamical system S1 can be embedded in the dynamical system S1-S2 featuring dihedral symmetry. **Figure 2A**. The S1's two-dimensional planar layer contains a family of Hamiltonian level curves indexed by energy $\alpha \in (0, 1)$. Looking just at S1, the changes in energetic levels are interpreted as isolated. **Figure 2B-D**. S1 in not any more an isolated manifold, but rather is embedded in a three-dimensional system that contains also the perpendicular hidden subsystem S2. The S1-S2 system corresponds to the manifold illustrated in **Figure 1F**. By increasing or decreasing the α value, different predictable time dynamics are achieved in every single subsystem (thicker circles in **Figures 2B**, **2C**, **2D**). Contrary to the subsystem S1, the S2's energetic values decrease from the center to the periphery, so that energetic changes in S1 are inversely proportional to changes in S2. Modified from Klee (2018b); Klee (2019). **Figure 2E**. A three-dimensional reconstruction of the S1-S2 system (α=0.61).

APPLICATIONS OF HYPERGEOMETRIC PERIODIC FUNCTIONS TO PHYSICAL AND BIOLOGICAL SYSTEMS

Feasible physical and biological PFHM applications are suggested in the sequel. The toric sections of the Hamiltonian described above can be examined in terms of forces able to influence the dynamics of the system under assessment. The PFHM homoclinic orbits could represent the energetic levels of physical forces like gravitation or electromagnetism, the trajectories of particles moved by mechanical forces, biological diffusion mechanisms, the paths followed by social agents' networks, etc. Here follows a list of examples introducing physical and biological systems in terms of PFHM-like paths.

Hidden energetic constraints. The dynamics of physical and biological systems are usually tackled by envisioning the intrinsic and extrinsic forces that constrain the phase spaces trajectories. For instance, fluctuating colloidal nanoclusters can be driven to reach an arbitrary target shape by properly setting a macroscopic external field (Boccardo and Pierre-Louis, 2022). To provide another example, the mechanical response of sub-100 nm scale materials is deeply influenced by the termination lines of the boundaries at the solid surface where the crystalline grains meet (Zhang et al., 2021). The PFHM approach suggests that the energetic levels of certain thermodynamic paths occurring in seemingly isolated dynamical systems could be influenced by hidden factors, even in the absence of accurate knowledge of the systems parameters. This means that thermodynamic accounts must consider not just of the system under evaluation, but also its potential co-joined systems. In touch with this suggestion, concerning the conformational fluctuations of whole protein structures, the external occurrence of water molecules between protein domains is mandatory to induce large-amplitude motions of multi-domain proteins (Oroguchi and Nakasako, 2016). In a PFHM framework of protein domains, microscopic changes in hidden subsystems (i.e., changes in local hydration of hydrophobic pockets or hydrophilic crevices in the clefts) lead to macroscopic changes in the whole system (i.e., domain motions' switches).
We argue that nonequilibrium dynamical systems' perturbative phenomena like heterogeneities and the existence of multiple stable states (Briske et al., 2017), together with dissipative forces like internal friction and material loss, could be evaluated in terms of PFHM. This suggests that driving forces from hidden coupled subsystems may lead to energetic changes in the system under assessment.

In a PHFM dynamical system, the energy tends to an energetic value that must be balanced between the subsystems that make it up. In the example illustrated in **Figures 1F** and **2**, the coupled subsystems S1 and S2 are correlated by an inverse linear function in such a way that the total energy of the whole system must be preserved. When the S1's energy tends to zero, the S2 energy must tend to 1, and vice versa. Since these dynamics result in linear, balanced, reciprocally induced energetic constraints between the S1 and S2 subsystems, the whole system S1-S2 is forbidden to achieve a final configuration that simultaneously minimizes all interaction energies. Therefore, S1 and S2 cannot simultaneously display the highest and the lowest energetic levels. This is the case of protein frustration, in which the least energetic point towards the maximum entropy conformation is almost never reached due to the presence of accidental degeneracy of ground states (Tozzi et al., 2016; Hanai 2024). Protein frustration's dynamics are reminiscent of PFHM-like systems, in which conflicting and entangled objectives do exist between the S1's and S2's dynamics. This leads to subsystems' reciprocal constraints that forbid the lowest-energy configuration theoretically achievable by the whole system. Both frustrated systems and reciprocally interacting hypergeometric coupled systems exhibit marginal orbits that can be regarded as the dynamical counterpart of accidentally degenerate ground states with symmetry breaks. Therefore, regardless of the gradient descent equations, the very occurrence of the coupled subsystems is able to restraint the ultimate energetic conformation of the whole system.

Phase spaces for quantum entanglement. In a PFHM-like phase space, the energetic configuration of particles located in a subsystem can be predicted by looking at the energetic configuration of particles located in the coupled subsystems, and vice versa. PFHM allows the description of the coordinate variables in terms of complex values matching each plane curve to a Riemann surface $\mathcal{S}(\alpha, \epsilon)$ with nontrivial topology. This observation provides the background to treat quantum dynamics' phenomena in terms of paths traveling inside PFHM-like manifolds. Especially, PHFM might deliver the mathematical and logical backbone to provide an explanation for the puzzling phenomenon of quantum entanglement (Krutyanskiy et al., 2023). The simultaneous correlation of two entangled particles makes sense if we consider them as embedded inside hypergeometric mathematical phase spaces where constrained trajectories like the ones described in **Figure 1** occur. Concerning the system illustrated in **Figures 1F** and **2**, a change in S1 must be coupled with a change in S2. The knowledge of the position of a particle located in the S1 subsystem allows the knowledge of the position of another particle located in the S2 subsystem. This means that modifications of an S1 particle lead to modifications in its S2 entangled particle. As suggested by Tozzi and Papo (2020), the very mathematical features of dynamical systems may naturally lead to physical events that are simultaneous and therefore devoid of the classical cause/effect relationships based on the temporal sequence of two events.
In a PHFM framework, the correlation between two entangled particles is mediated by the very structure of the coupled subsystems where the two particles are embedded. Entanglement becomes an external relation characterised by mutual

information (Cinti et al., 2022) between S1 and S2, in which trajectory changes in one spatial location lead to trajectory changes in another spatial location.

PFHM affects physical and biological paths. The dynamics described by Turing's reaction-diffusion model (henceforward RD) (Turing 1952) could be treated in terms of oscillations taking place inside PFHM-like phase spaces. In RD reactions, the balance and competition between excitatory and inhibitory inputs produces peculiar two-dimensional diffusion patterns of traveling substances (Kondo and Miura 2010) (**Figure 3A**). RD has been proven useful to describe the formation of self-organized patterns like leopard spots, zebrafish markings (Kondo et al., 2009), lung branching morphogenesis (Xu et al., 2017) and hippocampal grid cell's firing patterns (Deca 2017). We suggest that a PHFM approach might allow the assessment of RD-like patterns in three-dimensions (**Figure 3B**). To provide an example related with the PHFM system illustrated in **Figures 1F** and **2**, the concentric pattern generated by the subsystem S2 intersects the concentric pattern generated by the orthogonal subsystem S1. The reciprocal constraints generated by the interaction of the S1's and S2's diffusion waves might result in a three-dimensional dynamical system where RD could take place.

The various PFHM-like geometric shapes (like the triangles, the squares and the hexagons illustrated in **Figure 1**) exhibit striking similarities with the rich morphology of natural structures. For instance, morphological similarities occur between the structure of graphene and the hexagonal PHFM system illustrated in **Figure 3C**. The constant energy contour plot of the graphene's two-dimensional electronic band structure can be treated in terms of a hexagonal system S1. This means that the trigonal structures around the K points where the bands cross the Fermi level (energy E=0 eV) could be theoretically influenced by the energetic levels of the orthogonal structures outside the K points (Alfonsi, 2011) (**Figure 3C**). To provide another example, the atomic orbitals, i.e., the wavefunctions standing for the solutions of the Schrödinger equation for the atom (Gsaller 2007), when plotted in three dimensions exhibit characteristic shapes that resemble the conformation of PFHM coupled systems (**Figure 3D**).

PFHM-like mathematical functions could be also used to investigate various types of networks and graphs that are usually employed to describe social behaviors, since analogues between graph theory and theory of algebraic manifolds can be easily exploited (Bolker et al., 2002). In touch with this approach, many Boolean networks underlying biological regulatory networks (Schwab et al., 2020) could be treated in terms of different sets of states that evolve into closed cycles corresponding to PFHM-like basins of attraction. The behavior of social systems could be influenced by hidden factors located in PFHM-like hidden subsystems. These hidden subsytems might stand for ecological processes representing feedback mechanisms to moderate fluctuations of resilient communities in response to perturbing events (Briske et al., 2017).

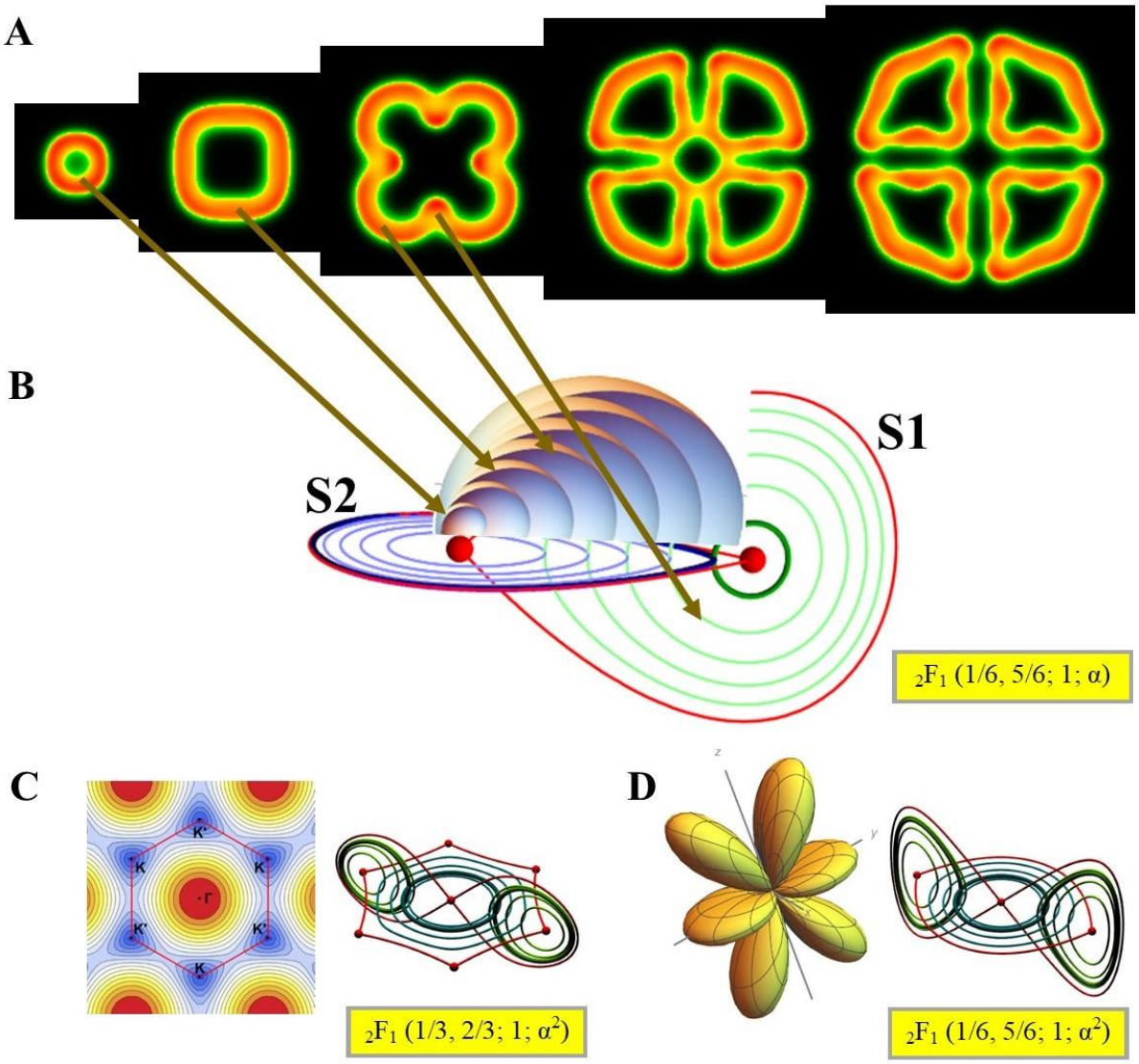

Figure 3A. Two-dimensional reaction diffusion system according to the Gray-Scott model (settings: feed rate = 0.037; death rate = 0.06). Modified from https://pmneila.github.io/jsexp/grayscott/ (retrieved May 5, 2024). **Figure 3B**. The two-dimensional reaction diffusion system is projected to the three-dimensional, PFHM S1-S2 system. The progressive homocyclic diffusion from S2 generates three-dimensional waves that, starting from the S2 center, diffuse towards the S2 periphery and the S1 center. When superimposition occurs between the two S1 and S2 orthogonal waves, the SD pattern is generated. Modified from Wolfram 2011.
Figure 3C. The hexagon of the two-dimensional Brillouin zone of a single graphene sheet displays similarities with the PFHM system illustrated in **Figure 1C**. Modified from Alfonsi (2011).
Figure 3D. The shape of the atomic orbital 4f (polynomial form $y z^2$) plotted in three dimensions displays similarities with similarities with the PFHM system illustrated in **Figure 1G**. Modified from Gsaller (2007).

Attractor-like gomboc dynamics. A PFHM approach may shed new light on well-known physical phenomena. A fixed point inside a PFHM could stand for the equilibrium point of a limit cycle where the derivatives of the coordinates are zero. The PFHM orbits could be treated not just as homocyclic curves, but also in terms of gradient flows tending towards stable nodes of nondegenerate minima. In this case, a peculiar fixed-point attractor is achieved on the compact PFHM manifold, where a maximum and a minimum are attained on a closed interval. In the example illustrated in **Figures 1F** and **2**, the S1 central point could represent both a limit-cycle attractor for the subsystem S1 and a bifurcation saddle point for the perpendicular subsystem S2. In this context, the mechanical behaviour of unusual bodies can be assessed in terms of PFHM. For instance, a monostatic body - like the toy "comeback kid"- is a rigid body subjected to gravity which displays on the horizontal surface just one stable equilibrium point (Chou and Friedman, 2016). The gomboc is a peculiar homogeneous three-dimensional, monostatic body with two equilibrium points, one stable and another unstable (Domokos et al., 1994; Varkonyi and Domokos, 2006). See **Figures 4A-4C** for further details. The differentiable function R(φ) denotes the boundary of the gomboc in a polar coordinate system (**Figure 4B**). The surface of the solid object displays R, which can be decomposed as follows:

$$R(\theta, \varphi, c, d) = 1 + d \cdot \Delta R(\theta, \varphi, c)$$

Where ΔR is the type of the deviation from the unit sphere, r, θ and φ denote the spherical coordinate system, R (θ,φ,c,d) is a family of surfaces, c>0 (≈0.275) is a parameter which controls the shapes of the thick and thin portions of the body (the smaller c, the closer to a tennis ball curve) and 0<d<1 is another parameter that must be very small ($d < 5 \times 10^{-5}$) to satisfy the convexity requirement. The formula suggests that the gomboc's dynamics are dictated by its very structure and shape.

The gomboc's single equilibrium point stands for the basin of attraction crossed with the aid of the gravitation, i.e., the external force able to restraint the converging paths towards the local minimum. Since the gomboc reaches its final stable configuration when the gravity is not counteracted by any mechanical force, a parallelism can be drawn with the above-mentioned S1-S2 system (**Figure 4E**). The fixed point in S1 is reached when the S1 energy is zero and the S2 energy is 1 (**Figure 4F**). In touch with the PFHM system in which the subsystems display inverse proportional energy, the gomboc's minimum energetic level is achieved when the maximum effect of the gravitational force is not anymore balanced by opposite mechanical forces.

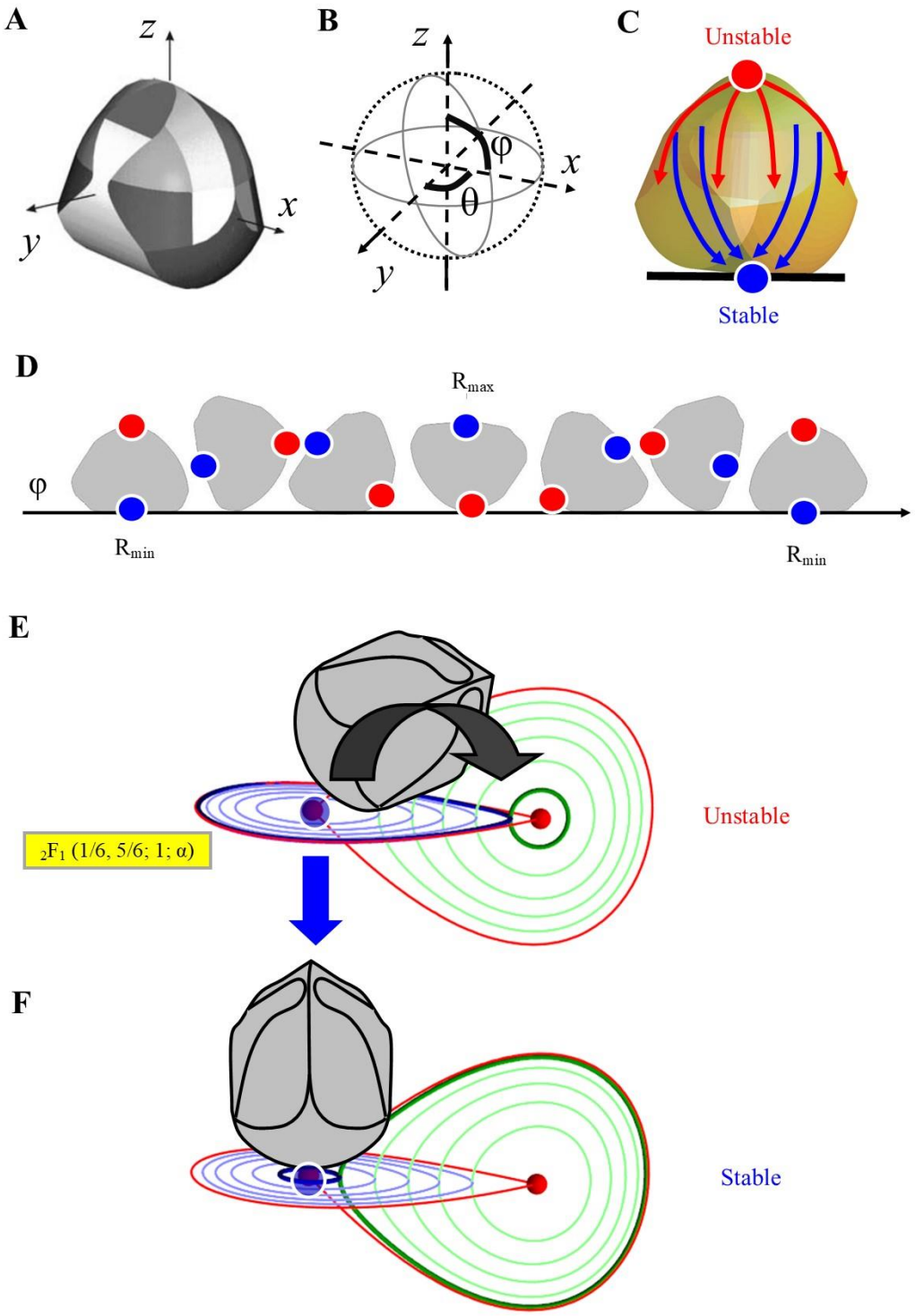

Figure 4A. A monostatic three-dimensional object (termed gomboc) equipped with a single point of stable equilibrium. **Figure 4B**. The gomboc can be embedded inside a spherical polar coordinate system with the origin at the center of gravity of the body. The three-dimensional body can be defined by the function $R(\phi,\Theta)$. **Figure 4C**. The gomboc displays the unique feature to be equipped with just one stable and one unstable point (blue and red spots, respectively). **Figure 4D**. The gomboc's movements lead to different intermediate paths. No matter how the gomboc is turned, it will always reach its single stable fixed point. R_{max} stands for the point of unstable equilibrium with the highest energy, while R_{min} for the stable point with the lowest energy. Modified from Domokos and Várkonyi (2008).
Figures 4E-F. The gomboc's movements can be described in terms of trajectories taking place inside the PHFM illustrated in **Figures 1F** and **2**. When the mechanical forces counteract and overtake the gravity, the gomboc moves following established trajectories (**Figure 4E**). When the gravity exerts its maximum force and the mechanical forces dissipate, the gomboc reaches its final, stable configuration (**Figure 4F**).

CONCLUSIONS

We explored the idea of algebraic and/or geometric structures subtending the phase spaces of physical and biological dynamical systems. This mathematical framework for real dynamics has been already considered by many scientists. For instance, it has been suggested that the three-dimensional cubic surface $Va,b,c,d(x,y,z)$ correlated with the dynamical (non-linear and transcendental) Painlevé VI equation paves the way to an approach to DNA/RNA sequences in which essential singularities remain fixed during poles shift (Planat et al., 2024). In our paper, we focused on a peculiar hypergeometric manifold, inspired by the versatile PF. This approach generates coupled systems composed of visible and concealed subsets with energetic interactions that are reciprocal in nature.
Many clues suggest that PFHM could be used to investigate real dynamics. It is noteworthy that the homoclinic orbits and global bifurcations like the ones described by PFHM can be identified in many physical and biological tracks (Chen et al., 2018). In astronomy, certain basic homoclinic and periodic orbits have been used to analyze planar equilateral restricted four-body problems in terms of conservative autonomous vector fields (Hetebrij and Mireles James, 2021). An atlas has been provided of the stable/unstable manifolds attached to an equilibrium point, in order to assess not just the maximally symmetric case of equal masses, but also the symmetry breaks leading to connecting orbits of nonequal masses (Kepley and Mireles James, 2019). Further, saddle-node dynamics have been studied in Lorenz systems, suggesting that infinite homoclinic orbits are associated with unstable periodic motions and period-doubling bifurcation trees towards chaos (Guo et al., 2021). The last, but not the least, the central nervous system displays heteroclinic sequential dynamics that can be expressed in the form of kinetic equations (Rabinovich and Varona, 2011).

Summarizing, different features of PHFM could be used to tackle various physical and biological dynamics:

1) The constrained inverse reciprocity of the trajectories in coupled subsystems could be used to assess quantum entanglement.
2) The system's requirements of energy conservation could be used to assess frustrated systems.
3) The possibility to treat PHFM in terms of cycle attractors could be used to assess unusual dynamical systems like the gomboc.
4) The possibility to describe systems' energetic dynamics in a more extrinsic way could be used to assess the unnoticed presence of hidden coupled systems.
5) The possibility to treat two-dimensional systems in terms of three-dimensional systems could be used to investigate the ubiquitous Turing's reaction-diffusion model according to an unfamiliar three-dimensional perspective.

PFHMs display other features that have not been covered here and that could be useful for the evaluation of real systems dynamics. For instance, another property could be explored that is ubiquitous in physical and biological systems, i.e., the possibility that the homocyclic orbits could run clockwise or counterclockwise. Still, the fact that PFHMs are formed by two-dimensional systems that are perpendicular is worth exploring, since many real systems are characterized by the occurrence of orthogonal planes. For example, the interaction of transverse/longitudinal electrical and magnetic fields with charged particles produces particle acceleration in beam transport systems (Wiedemann 2015; Sánchez et al., 2023). These synchrotron oscillations' dynamics could be described in terms of PFHM systems under various initial conditions, including unstable motion and potential well for moving radiofrequency buckets. A PFHM approach could also be methodologically useful to elucidate quantum features of quasiparticles like phonons, magnons and anyons. In condensed matter physics, a quasiparticle stands for the collective behavior of a group of particles that can be treated as if they were a single particle, since the motion of many particles behaves like a single entity equipped with collective excitations (Verresen et al. 2019). Another feasible PFHM application concerns the possibility to explore the relationship between different manifolds' trajectories in terms of mappings and projections. With the aid of higher-dimensional Poincaré maps, two- and three-dimensional routes could be used to compute resonant orbits in the Earth–Moon restricted problem (Vaquero and Howell, 2014). We suggest that a message (or a visual image) incorporated in the PFHM subsytems' invariant orbits can be mapped to the orbits of another subsystem, achieving a hypergeometric projection of the original message. Like the charting of a world map, homoclinic/heteroclinic-type projections between two coupled hypergeometric manifolds can be accomplished, with applications in digital imaging, cryptography and memory storing.

REFERENCES

1) Alfonsi, Jessica. 2011. Optical Properties of Graphene. http://demonstrations.wolfram.com/OpticalPropertiesOfGraphene/ Wolfram Demonstrations Project
2) Becken W, P. Schmelcher. 2000. The analytic continuation of the Gaussian hypergeometric function 2F1(a,b;c;z) for arbitrary parameters. Journal of Computational and Applied Mathematics. Volume 126, Issues 1–2, 30 December 2000, Pages 449-478
3) Beukers Frits; Gert Heckman. 1989. Monodromy for the hypergeometric function nFn-1. Invent. Math. 95 (1989) 325-354,
4) Boccardo, Francesco; Olivier Pierre-Louis. 2022. Controlling the Shape of Small Clusters with and without Macroscopic Fields. Phys. Rev. Lett. 128, 256102 – Published 22 June 2022
5) Bolker, Ethan; Victor Guillemin, Tara Holm. 2002. How is a graph like a manifold? arXiv:math/0206103
6) Briske, D.D., Illius, A.W., Anderies, J.M. (2017). Nonequilibrium Ecology and Resilience Theory. In: Briske, D. (eds) Rangeland Systems. Springer Series on Environmental Management. Springer, Cham. https://doi.org/10.1007/978-3-319-46709-2_6
7) Chen, Y., Wu, T. & Yang, X. On the existence of homoclinic orbits in some class of three-dimensional piecewise affine systems. Comp. Appl. Math. 37, 6022–6033 (2018). https://doi.org/10.1007/s40314-018-0659-6
8) Chou C-S, Friedman A. 2016. System of Two Linear Differential Equations. Introduction to Mathematical Biology pp 29-42.
9) Cinti, E., Corti, A. & Sanchioni, M. 2022. On entanglement as a relation. Euro Jnl Phil Sci 12, 10. https://doi.org/10.1007/s13194-021-00439-5
10) Deca D. 2017. Grid Cells-From Data Acquisition to Hardware Implementation: A Model for Connectome-Oriented Neuroscience. In: The Physics of the Mind and Brain Disorders: Integrated Neural Circuits Supporting the Emergence of Mind, edited by Opris J and Casanova MF. New York, Springer; Series in Cognitive and Neural Systems. Pages 493-511. ISBN: 978-3-319-29674-6.
11) Domokos G, Papadopulos J, Ruina A. 1994. Static equilibria of planar, rigid bodies: is there anything new? Journal of Elasticity volume 36, 59–66.
12) Domokos G, Várkonyi P. 2008. Geometry and self-righting of turtles. Proc. R. Soc. B.27511–17. http://doi.org/10.1098/rspb.2007.1188
13) Hetebrij, Wouter; J. D. Mireles James. 2021. Critical homoclinics in a restricted four-body problem: numerical continuation and center manifold computations. Celestial Mechanics and Dynamical Astronomy. Volume 133, article number 5.
14) Fürnsinn Florian; Sergey Yurkevich. 2023. Algebraicity of hypergeometric functions with arbitrary parameters. arXiv:2308.12855
15) Gsaller, Guenther. 2007. Visualizing Atomic Orbitals. http://demonstrations.wolfram.com/VisualizingAtomicOrbitals/ Wolfram Demonstrations Project
16) Hanai, Ryo. 2024. Nonreciprocal Frustration: Time Crystalline Order-by-Disorder Phenomenon and a Spin-Glass-like State. Phys. Rev. X 14, 011029 – Published 26 February 2024
17) Guo, S., Luo, A.C. A Family of Periodic Motions to Chaos with Infinite Homoclinic Orbits in the Lorenz System. Lobachevskii J Math 42, 3382–3437 (2021). https://doi.org/10.1134/S1995080222020093
18) Jong, Mathijs de; Seijo, Luis; Meijerink, Andries; Rabouw, Freddy T. 2015. Resolving the ambiguity in the relation between Stokes shift and Huang–Rhys parameter. Physical Chemistry Chemical Physics. 17 (26): 16959–16969. doi:10.1039/C5CP02093J.
19) Kepley, Shane; J. D. Mireles James. 2019. Homoclinic dynamics in a restricted four-body problem: transverse connections for the saddle-focus equilibrium solution set. Celestial Mechanics and Dynamical Astronomy. Volume 131, article number 13.
20) Klee, Brad. 2018a. Deriving Hypergeometric Picard-Fuchs Equations. http://demonstrations.wolfram.com/DerivingHypergeometricPicardFuchsEquations/ Wolfram Demonstrations Project.
21) Klee Brad. 2018b. D4 Symmetric Stratum of Quartic Plane Curves. http://demonstrations.wolfram.com/D4SymmetricStratumOfQuarticPlaneCurves/ Wolfram Demonstrations Project
22) Klee, Brad. 2019. A Few More Geometries after Ramanujan. http://demonstrations.wolfram.com/AFewMoreGeometriesAfterRamanujan/ Wolfram Demonstrations Project.
23) Kondo S, Iwashita M, Yamaguchi M. 2009. How animals get their skin patterns: fish pigment pattern as a live Turing wave. Int J Dev Biol. 2009;53(5-6):851-6. doi: 10.1387/ijdb.072502sk.
24) Kondo S, Miura T. 2010. Reaction-diffusion model as a framework for understanding biological pattern formation. Science. 2010 Sep 24;329(5999):1616-20. doi: 10.1126/science.1179047.
25) Kreshchuk, Michael; Tobias Gulden 2019 J. Phys. A: Math. Theor. 52 155301. DOI 10.1088/1751-8121/aaf272
26) Krutyanskiy, V; M. Galli, V. Krcmarsky, S. Baier, D. A. Fioretto, et al. 2023. Entanglement of Trapped-Ion Qubits Separated by 230 Meters Phys. Rev. Lett. 130, 050803 – Published 2 February 2023

27) Mickens, R.E. 1979. Long-range interactions. Found Phys 9, 261–269. https://doi.org/10.1007/BF00715182
28) Xu H Sun M, Zhao X. 2017. Turing mechanism underlying a branching model for lung morphogenesis. PLoS One. 2017 Apr 4;12(4):e0174946. doi: 10.1371/journal.pone.0174946.
29) Olde Daalhuis AB. 2010. Hypergeometric function. In Olver, Frank W. J.; Lozier, Daniel M.; Boisvert, Ronald F.; Clark, Charles W. (eds.), NIST Handbook of Mathematical Functions, Cambridge University Press, ISBN 978-0-521-19225-5, MR 2723248.
30) Oroguchi, T., Nakasako, M. 2016. Changes in hydration structure are necessary for collective motions of a multi-domain protein. Sci Rep 6, 26302 (2016).
31) Planat, Michel; David Chester, Klee Irwin. 2024. Dynamics of Fricke–Painlevé VI Surfaces. Dynamics 2024, 4(1), 1-13; https://doi.org/10.3390/dynamics4010001
32) Rabinovich, Mikhail I; Pablo Varona. 2011. Robust transient dynamics and brain functions. Front. Comput. Neurosci., 13 June 2011. volume 5 - 2011 | https://doi.org/10.3389/fncom.2011.00024
33) Ramanujan S. 1914. Modular Equations and Approximations to π,". *Quarterly Journal of Mathematics*, **45**, 1914 pp. 350–372.
34) Ratner, Schatz; Mark A., George C. (2001). Quantum Mechanics in Chemistry. 0-13-895491-7: Prentice Hall. pp. 90–91.
35) Sánchez, E.A., Flores, A., Hernández-Cobos, J. et al. 2023. Increasing beam stability zone in synchrotron light sources using polynomial quasi-invariants. Sci Rep 13, 1335 (2023). https://doi.org/10.1038/s41598-023-27732-y
36) Schwab, Julian D; Silke D. Kühlwein, Nensi Ikonomi, Michael Kühl, Hans A. Kestler. 2020. Concepts in Boolean network modeling: What do they all mean? Computational and Structural Biotechnology Journal. Volume 18, 2020, Pages 571-582. https://doi.org/10.1016/j.csbj.2020.03.001
37) Shen, L. C. 2017. On Three Differential Equations Associated with Chebyshev Polynomials of Degrees 3, 4 and 6. Acta Mathematica Sinica, 33(1), 2017 pp. 21–36. doi:10.1007/s10114-016-6180-1.
38) Tozzi A, Fla Tor, Peters JF. 2016. Building a minimum frustration framework for brain functions in long timescales. J Neurosci Res. 94(8): 702–716.
39) Tozzi A, Papo D. 2020. Projective mechanisms subtending real world phenomena wipe away cause effect relationships. Progress in Biophysics and Molecular Biology. 151:1-13. DOI: 10.1016/j.pbiomolbio.2019.12.002.
40) Turing AM. 1952. The chemical basis of morphogenesis. Philos Trans R Soc B; Biol Sci 237(641): 37-73.
41) Vaquero, Mar; Kathleen C. Howell. 2014. Design of transfer trajectories between resonant orbits in the Earth–Moon restricted problem. Acta Astronautica, Volume 94, Issue 1, January–February 2014, Pages 302-317 https://doi.org/10.1016/j.actaastro.2013.05.006
42) Varkonyi PL, Domokos G. 2006. Static Equilibria of Rigid Bodies: Dice, Pebbles, and the Poincare-Hopf Theorem. Journal of Nonlinear Science volume 16, 255–281.
43) Verresen, R., Moessner, R. & Pollmann, F. Avoided quasiparticle decay from strong quantum interactions. Nat. Phys. 15, 750–753 (2019). https://doi.org/10.1038/s41567-019-0535-3
44) Wiedemann, H. 2015. Longitudinal Beam Dynamics. In: Particle Accelerator Physics. Graduate Texts in Physics. Springer, Cham. https://doi.org/10.1007/978-3-319-18317-6_9
45) Wolfram S. 2011. Waves from a Moving Source in 3D. Wolfram Demonstrations Project. http://demonstrations.wolfram.com/WavesFromAMovingSourceIn3D/
46) Zhang, Ye-Yuan; Hui Xie, Ling-Zhi Liu, and Hai-Jun Jin. 2021. Surface Triple Junctions Govern the Strength of a Nanoscale Solid. Phys. Rev. Lett. 126, 235501.